

**Four-decade record of pervasive grounding line retreat along the Bellingshausen  
margin of West Antarctica**

Frazer D.W. Christie<sup>1</sup>, Robert G. Bingham<sup>1</sup>, Noel Gourmelen<sup>1</sup>, Simon F.B. Tett<sup>1</sup>, Atsuhiko  
Muto<sup>2</sup>

<sup>1</sup> School of GeoSciences, University of Edinburgh, UK

<sup>2</sup> Department of Earth and Environmental Science, Temple University, USA

*Corresponding Author:* Frazer Christie, F.Christie@ed.ac.uk

**Key Points**

- Grounding line change mapped along Bellingshausen margin of West Antarctica with Landsat and InSAR from 1975 to 2015
- Results show majority of grounding line retreated along entire margin implicating ocean-forced dynamic thinning
- Grounding line at Venable Ice Shelf currently pinned but potential for retreat as at Pine Island Glacier

This article has been accepted for publication and undergone full peer review but has not been through the copyediting, typesetting, pagination and proofreading process which may lead to differences between this version and the Version of Record. Please cite this article as doi: 10.1002/2016GL068972

## **Abstract**

Changes to the grounding line, where grounded ice starts to float, can be used as a remotely-sensed measure of ice-sheet susceptibility to ocean-forced dynamic thinning. Constraining this susceptibility is vital for predicting Antarctica's contribution to rising sea levels. We use Landsat imagery to monitor grounding line movement over four decades along the Bellingshausen margin of West Antarctica, an area little monitored despite potential for future ice losses. We show that ~65% of the grounding line retreated from 1990-2015, with pervasive and accelerating retreat in regions of fast ice flow and/or thinning ice shelves. Venable Ice Shelf confounds expectations in that despite extensive thinning, its grounding line has undergone negligible retreat. We present evidence that the ice shelf is currently pinned to a sub-ice topographic high which, if breached, could facilitate ice retreat into a significant inland basin, analogous to nearby Pine Island Glacier.

## **Index Terms and Keywords**

0728 Ice shelves

0730 Ice streams

0758 Remote sensing

6924 Interferometry (1207, 1209, 1242)

9310 Antarctica (4207)

Landsat, InSAR, grounding line, Pine Island Glacier, Antarctica, ice-ocean interaction

## 1. Introduction

Satellite remote sensing of the Antarctic Ice Sheet over the last 25 years has revealed trends of ice loss that are especially pronounced around its coastline [*Shepherd et al., 2010; McMillan et al., 2014*]. Manifested by thinning of floating ice [e.g. *Paolo et al. 2015*], dynamic thinning of grounded ice [e.g. *Pritchard et al., 2009*], and rapid retreat of grounding lines [e.g. *Rignot et al., 2014*], these ice losses form one of the largest components of contemporary global sea-level rise [*Shepherd et al., 2012; Vaughan et al., 2013*]. However, the processes by which they occur remain imperfectly understood. The spatiotemporal distribution of the observed ice losses strongly suggests a forcing that initiates at ice-sheet margins [*Pritchard et al., 2012*], and several recent studies have attributed the dynamic thinning of grounded ice to the thinning of ice shelves [*Jenkins et al. 2010; MacGregor et al. 2012; Pritchard et al., 2012*]. This is, in turn, a possible consequence of the ingress of relatively warm circumpolar deep water (hereafter CDW) across the continental shelf to the sub-ice-shelf cavity [*Walker et al., 2007; Jacobs et al., 2011; Bingham et al., 2012*]. These processes are hypothesized to be responsible for ice losses from the sectors of West Antarctica that drain to the Amundsen and Bellingshausen Seas [*Rignot et al., 2008; Pritchard et al., 2012; Bingham et al., 2012*] but, while the former has received considerable observational and modelling attention [*Payne et al., 2004; Shepherd et al., 2004; Scott et al., 2009; Joughin et al., 2012; Favier et al., 2014; Joughin et al., 2014; Rignot et al., 2014; Seroussi et al., 2014; Goldberg et al., 2015*], few observations of glacial change in the Bellingshausen Sea Sector (hereafter BSS) have been published.

It is important to generate improved records of glacial change in the BSS for several reasons. First, the estimated mass lost from the region between 1992 and 2006 ( $\sim 49 \text{ Gt yr}^{-1}$ ) comprised

35% of total mass loss from the West Antarctic Ice Sheet [Rignot et al., 2008], second only to contributions from the Amundsen Sea Sector (~64 Gt yr<sup>-1</sup>; 46% of total loss). Second, a recent study has suggested that mass loss since 2009 has been particularly significant, and that the region may have destabilised [Wouters et al., 2015]. Third, although studies from the neighbouring Amundsen Sea Sector are offering insights into dynamic thinning and its possible oceanic forcing, the scarcity of glacial-change records and supporting information in the BSS (such as sub-shelf and grounded-ice geometry; physical oceanographic data) make it difficult to assess whether changes in the BSS have occurred at similar or different timescales to those in the Amundsen Sea Sector, potentially implicating different or additional forcing or feedbacks.

In order to improve our understanding of glacial change across this region, we generated a comprehensive dataset of grounding line (hereafter GL) positional change along the Bellingshausen Sea coastline for the period 1975-2015. We exploited a combination of optical and radar satellite imagery to map GL positions at approximately 5- to 10-year intervals. We find that, over this 40-year period, almost the entire length of the coastline has experienced GL retreat, with the greatest retreat typically occurring in regions containing deeply-bedded, fast-flowing outlet glaciers and ice streams. We suggest that this pervasive trend implicates widespread access of CDW to the Bellingshausen glacial margin, so that even despite relatively high accumulation inland, the mass balance for much of the region is strongly negative. Only in some special cases has the GL remained relatively stable in position or undergone advance, probably as a result of local topographic pinning that is likely to be overcome with continued regional oceanic forcing.

## 2. Methodology

### 2.1 Landsat grounding line mapping

We used Landsat optical satellite imagery as our primary data source due to its unmatched spatial-temporal coverage compared with other remote sensing datasets covering the BSS. The position of the GL was mapped from these images at 5- to 10-year intervals between 1975 and 2015 as follows.

Referring to the conceptual diagram of *Fricker et al.* [2009; their Fig. 2], the “true” GL (where ice decouples from the bed and begins to float due to tidal forcing; their “*G*”) cannot be identified reliably with static, optical imagery (such as Landsat). Instead, using Landsat imagery, the most suitable proxy for *G* is the break-in-slope, otherwise known as the “inflexion point” [hereafter *I<sub>b</sub>*; after notation in *Fricker et al.*, 2009], which is defined as the most seaward continuous slope break detectable in satellite imagery [*Brunt et al.*, 2010; following *Scambos et al.*, 2007]. Situated within close proximity to *G*, *I<sub>b</sub>* appears as a clearly defined shadow-like change in image brightness on optical imagery [cf. *Bindschadler et al.*, 2011] (Figure S1).

Using GIS tools on georeferenced multispectral Landsat scenes (Table S1), we digitised the position of *I<sub>b</sub>* at approximately 50-100 m intervals along the BSS coastline and coastal islands for years 1975, c.1985, c.1990, 2000, 2005, 2010 and 2015. The majority of scenes used were acquired during austral summer (January/February). For c.1985 and c.1990 we utilized data from  $\pm 2$  years where 1985/1990 scene spatial coverage was poor. Throughout the study, only images with cloud cover  $\leq 10\%$  were utilized. The launch failure of Landsat 6 in 1993 was

responsible for a hiatus in Landsat acquisitions throughout the mid-1990s, precluding any mapping of results for c.1995.

Using a similar  $I_b$  mapping technique to that employed by *Bindschadler et al.* [2011], we estimate positional uncertainty ( $1\sigma$ ) of  $I_b = \sim 103$  m for most of the BSS coastline (206 m for 1975 mapping), with the exception of the fast-flowing Ferrigno Ice Stream, where  $I_b (1\sigma) = \sim 502$  m (cf. *Bindschadler et al.* [2011]; see Text S1, Table S2). In terms of the principal objective of this paper, which is to monitor changes in the position of the GL across 5-year intervals, any imprecision in locating  $I_b$  (on the order of  $10^2$  m) is outweighed by changes in its position after 5 years (on the order of  $10^2$ - $10^3$  m). This uncertainty broadly matches the positional uncertainty associated with other remote sensing techniques, such as Interferometric Synthetic Aperture Radar [InSAR; cf. *Rignot et al.*, 2011].

It is important to recognise that under some conditions the use of  $I_b$  as a proxy for the GL may fail [cf. *Fricker et al.*, 2009]. The typical contexts in which  $I_b$  makes a poor indicator are in areas of fast ice flow, where subglacial bed and surface slopes are shallow and  $I_b$  is difficult to define; and/or in ice plains, where multiple breaks-in-slope may be present around the grounding zone, or where the break-in-slope may decouple substantially from the location of the “true” GL with tidal variability [cf. *Corr et al.*, 2001; *Fricker & Padman*, 2006; *Fricker et al.*, 2009; *Brunt et al.*, 2011]. Therefore, to ascertain the utility of Landsat for monitoring GL change, we additionally employed InSAR mapping techniques to monitor the nature and configuration of grounding zones throughout the BSS, and to identify the potential presence of ice plains in this sector.

## 2.2 Interferometric Synthetic Aperture Radar (InSAR)

Where Synthetic Aperture Radar (SAR) observations have been acquired, it is possible to map the inland limit of tidal flexure acting on the grounding zone,  $F$ , directly [e.g. *Fricker et al.*, 2009; their Figure 2; *Brunt et al.*, 2010; *Rignot et al.*, 2011]. We applied interferometry to SAR data acquired from the European Space Agency's ERS-1 and ERS-2 satellites to delineate  $F$  along the BSS coastline between 1992 and 2011. The data consist of SAR scenes acquired in 1992, 1994, 1996 and 2011 (Table S4), and the generated interferograms have temporal baselines of either 1 day (1996) or 3 days (1992, 1994, 2011).

Following *Park et al.* [2013], we employed a double-differential InSAR processing technique, whereby we differenced consecutive interferograms, corrected for the effects of surface topography using a resampled version of the Bedmap2 surface digital elevation model [*Fretwell et al.*, 2013], in order to remove signals related to ice flow and reveal vertical surface motion due to tidal flexure acting upon the grounding zone from floating ice shelves. Such motion, which is represented in double-differenced interferograms as a band of closely spaced fringes across the grounding zone (Figure S2), reveals  $F$  as the landward limit of tidally-induced vertical ice motion.

To quantify the positional uncertainty of InSAR-derived  $F$ , we compared the tidally-variable location of  $F$  from multiple double-differenced interferograms, where possible across multiple epochs. From this, we estimated tidally-induced variation in  $F$  to range from  $\sim\pm 100$  m across areas of steeply-bedded, shoaling subglacial topography to  $\leq \sim\pm 300$  m across deeply-grounded outlet glaciers with shallow bed slopes. These values align with positional accuracy estimations in other areas of Antarctica (cf. *Rignot et al.* [2011]; *Park et al.* [2013]).

Our determination of InSAR-derived  $F$  confirms the absence of ice plains and other complex ice-shelf geometries along the BSS. Therefore, unlike for other regions of Antarctica where optical based  $I_b$  mapping campaigns have been prone to failure (e.g. *Fricker et al. [2009]*; *Brunt et al. [2011]*), we are confident that Landsat-derived  $I_b$  acts as a good proxy for the GL in this sector.

### 2.3 Quantifying grounding line position retreat/advance

To quantify GL advance or retreat over epochs, we defined the 2015 Landsat-mapped  $I_b$  as a baseline. We partitioned this baseline into 30-km segments, and at the limit of each segment defined a normal extending infinitely both landward and seaward from the baseline. These normals intercept the mapped  $I_b$  for all years. To calculate advance or retreat of  $I_b$  for any 30 km segment of coastline over any period [2015 –  $y$ ], where  $y$  = year of interest, we defined a polygon bounded by the 2015 baseline, the mapped  $I_b$  for year  $y$ , and the two intercepting normals. We then summed the areas of each polygon, in each case defining whether  $I_b$  had retreated or advanced over the epoch of interest; and then divided by 30 km to convert the final figure into a magnitude of  $I_b$  advance/retreat over each epoch of interest (see Text S2 and Data Set S1).

## 3. Results

[INSERT FIG. 1 & CAPTION]

Figure 1 shows that the most significant changes to the GL position between 1990 and 2015 are located at Ferrigno and Fox Ice Streams ( $-2.77 \pm 0.50$  km and  $-1.79 \pm 0.14$  km

respectively) and Stange Ice Shelf ( $-0.92 \pm 0.14$  km). Since 1990, net GL retreat has been widespread along the BSS coastline and around Thurston Island, and has occurred along much of the margin draining to the Amundsen Sea between the Cosgrove Ice Shelf and Pine Island Glacier. In total, between 1990 and 2015, 65.4% of the GL along the mainland BSS experienced net retreat, and only 7.4% net advance. Over the same epoch, 29.3% of the GL around Thurston Island experienced net retreat, and only 1.8% net advance. Most of the detectable retreat around Thurston Island occurred along its southern (Abbot Ice Shelf-facing) margin; change along its northern margin was often not possible to discern outside Landsat 1 $\sigma$ -error bounds. Figure 1 also shows the tendency for the greatest GL retreat to be associated with regions of fast-flowing, likely deeply-grounded ice.

**[INSERT FIG. 2 & CAPTION]**

Partitioning the observations into change over 5- to 10-year epochs (Figure 2), the most comprehensive coverage along the entire coastline begins in 1990, from which time it is clear that the pace of GL retreat at Eltanin Bay has been persistently high. There (for segments 22-26 in Data Set S1; locations of Ferrigno and Fox Ice Streams), the GL retreated on average  $0.45 \pm 0.14$  km (at a rate of  $45 \pm 27$  m yr<sup>-1</sup>) from 1990-2000,  $0.46 \pm 0.14$  km ( $92 \pm 27$  m yr<sup>-1</sup>) from 2000-2005,  $0.50 \pm 0.14$  km ( $100 \pm 27$  m yr<sup>-1</sup>) from 2005-2010, and most recently  $0.52 \pm 0.14$  km ( $104 \pm 27$  m yr<sup>-1</sup>) from 2010-2015.

Where data exist from 1975 or 1985 onwards, some sites experienced relatively fast GL retreat in the earlier epochs we have analysed, followed by slower retreat or undetectable change, and then increased retreat towards the present-day. One example is the western Stange Ice Shelf, where the GL at Berg Ice Stream retreated  $0.54 \pm 0.14$  km ( $36 \pm 27$  m yr<sup>-1</sup>)

between 1975-1990, remained stable within Landsat error bounds between 1990-2010, then retreated  $0.24 \pm 0.14$  km ( $48 \pm 27$  m yr<sup>-1</sup>) between 2010 and 2015. Further west, between latitudes 93°W (eastern Abbot Ice Shelf) and 87°W (Wiesnet Ice Stream/Venable Ice Shelf) we also find notable GL retreat between 1985 and 1990 relative to all intervening epochs until 2010-2015. In 2010-2015, the GL along eastern Abbot Ice Shelf then experienced a renewed retreat (distance  $0.31 \pm 0.14$  km; rate  $62 \pm 27$  m yr<sup>-1</sup>; segments 38-40 in Data Set S1), while the GL also experienced a detectable minor retreat between the Wiesnet and Williams Ice Streams feeding Venable Ice Shelf ( $0.23 \pm 0.14$  km at  $45 \pm 27$  m yr<sup>-1</sup>; segments 30 in Data Set S1).

#### **4. Discussion**

Our observations demonstrate that since 1975/1985 there has been a net retreat of the grounding line along almost all of the BSS (Figure 1; Figure 2; Figure S3), demonstrating a pervasive trend of ice response along the whole Bellingshausen Sea coastline. Within this trend, several further phenomena are notable. First, both the greatest retreat (Figure 1) and the greatest increase in GL retreat rates from the 1990s to the present (Figure 2) have occurred along the eastern BSS coast, incorporating the glaciers and ice streams draining to Eltanin Bay and Stange Ice Shelf. Second, observed retreat rates in the BSS have varied over time across different locations. Third, whilst the ice streams feeding the Venable Ice Shelf have experienced limited retreat over the last three decades, retreat rates do not align with the more pronounced glaciological changes occurring more widely across the BSS and nearby Amundsen Sea Embayment.

Ferrigno Ice Stream, where we have observed the greatest net GL retreat from 1990-2015 (Figure 1), has been highlighted in several previous studies as a region of especially pronounced ice-surface lowering and inferred ice loss [Rignot et al., 2008; Pritchard et al., 2009; McMillan et al., 2014; Wouters et al., 2015]. Bingham et al. [2012] suggested that Ferrigno Ice Stream is currently undergoing dynamic thinning as a consequence of the ingress of warm CDW to its ice front along Belgica Trough, a continental-shelf transecting depression formed during glacial maximum conditions [Ó Cofaigh et al., 2005; Figure 1]. Here we add that the GL of Ferrigno Ice Stream has been retreating since at least 1975 (Figure S3), and that the neighbouring Alison and Fox Ice Streams have been retreating since at least 1990 (Figure 2, Figure S3; no data exist beforehand), suggesting that the effects of CDW forcing have been prevalent in Eltanin Bay for at least twenty-five years. The region's vulnerability is likely exacerbated by shallow bed slopes observed near/at the grounding zones of this sector as compared to neighbouring regions [Bingham et al., 2012; Figure 3], in addition to the lack of an ice shelf to provide a backstress to grounded ice. As such, the general absence of ice shelves throughout this region further signals potentially longstanding ingress of CDW to the bay [Holland et al., 2010]. It is also notable that GL retreat here has occurred at a greater rate over the last decade (2005-2015) than previously (Figure 2); a trend which is in general agreement with those reported by Rignot et al. [2008], Pritchard et al. [2009], McMillan et al. [2014] and Wouters et al. [2015] with respect to other indicators of accelerating glacial response over this period. Moreover, following the approach of Park et al. [2013], GL thinning estimates obtained from our 2010-2015 GL retreat rates are consistent with estimates of inland thinning produced through CryoSat-2 swath processing over the same observational period (Figure S4, Text S3). Analysis of CryoSat-2-derived rates of surface elevation change reveals extensive thinning inland of the Fox and Ferrigno GLs (max.  $-6.40 \text{ m yr}^{-1}$ ,  $\sigma = \pm 0.49 \text{ m yr}^{-1}$ ), which compares well with our Landsat-derived theoretical

thinning estimations (mean =  $-5.96 \text{ m yr}^{-1}$ ,  $\sigma = \pm 3.40 \text{ m yr}^{-1}$ ; Figure S4, Text S3). There is therefore mounting evidence that the Eltanin Bay component of the BSS is not only prone to marine instability, but is already experiencing the early stages of retreat, like nearby Pine Island Glacier [cf. *Jenkins et al.* 2010].

**[INSERT FIG. 3 & CAPTION]**

Ice flowing into Stange Ice Shelf is also remarkable for experiencing extensive GL retreat since 1975 (Figure 2; Figure S3). The pervasiveness and magnitude of GL retreat there suggest that the ice shelf's capacity to buttress the contributing glaciers' flow has been diminishing as a likely consequence of ice-shelf thinning. Thinning across Stange Ice Shelf has been inferred from radar altimetry between 1992 and 2008 [*Holt et al.*, 2014] and 1994 to 2012 [*Paolo et al.*, 2015], though the rates have varied considerably with location and time [*Holt et al.*, 2014]. The greatest thinning of Stange Ice Shelf has consistently occurred on its westward flanks [*Paolo et al.*, 2015], but where the western Stange Ice Shelf meets the BSS GL (at Berg Ice Stream, Figure 1), GL retreat between 1975 and 2015 has been suppressed relative to further east (Figure 1; Figure 2). An explanation for this apparent discrepancy lies in the geometry of the ice bed at the relative locations: a radar profile approximately following the GL along Stange Ice Shelf hints at a shallower bed, or bed protuberance, underlying Berg Ice Stream's GL compared with at the more eastern outlets feeding the ice shelf (notably Lidke Ice Stream; Figure 3). With respect to the temporal changes in GL retreat, the oscillatory nature of the observed retreat rates (i.e. instances of large-to-small-to-large retreat through time) corresponds with the suppression of ice-shelf thinning *Paolo et al.* [2015] measured for all BSS ice shelves from ~2000-2008 relative to the periods immediately preceding and succeeding it (i.e. 1994-2000; 2008-2012). That the GL retreat and ice-shelf

thinning trends follow a similar oscillatory pattern lends credence to the hypothesis that regional changes on and around Stange Ice Shelf are, as with Ferrigno Ice Stream, fundamentally driven by persistent CDW access to the ice-shelf cavity [cf. *Holt et al., 2014*]. Though the sub-shelf and near-ice-front bathymetry of Stange Ice Shelf remain poorly surveyed [*Graham et al., 2011*], the observed behaviour of the GL retreat is strongly suggestive that the ice shelf is underlain by a north-south-aligned deep bathymetric trough that allows CDW to flow from the Ronne Entrance beneath Stange Ice Shelf to the GL.

GL retreat observed along the margins of the Abbot and Cosgrove Ice Shelves, as well as on southern Thurston Island, has occurred in locations further from known regions of CDW ingress (Figure 1). However, most of the larger retreats in the western Bellingshausen Sea (e.g. Rosanova Glacier, Figure 1) took place where Bedmap2 [*Fretwell et al., 2013*] indicates deeply bedded grounding zones. Similar to Stange Ice Shelf, parts of this coastline exhibited some oscillatory behaviour, with the margin between 100°W and 94°W (including Rosanova Glacier) and 93°W and 89°W (eastern Abbot Ice Shelf) experiencing higher retreat in 1985-90 relative to any subsequent epoch until 2010-15, when further enhanced GL retreat was observed. Given these observations, we hypothesize that CDW-forced dynamic thinning is also occurring in many of these locations. The dearth of bathymetric data in the western BSS [*Graham et al., 2011*] leaves open the possibility that throughout the length of the Abbot Ice Shelf, there may be undiscovered access routes for CDW to reach GLs here. Indeed, there is compelling evidence from recently acquired aerogeophysical data that a tectonically-rifted basin underlies the majority of the ice shelf [*Cochran et al., 2014*], and that deep topographic lows may be present near the grounding lines of the eastern Abbot Ice Shelf (Figure 3).

The few cases of GL advance we have observed across the BSS are located where ice at the GL is thin and slow, and the bed steepens/shoals inland (Figure 1). For example, the small advances at King Peninsula (Figure 1; segments 59, 61 and 62 in Data Set S1) occurred where ice thickness is ~200-400 m and modelled depth-averaged ice velocities are  $< 100 \text{ m yr}^{-1}$ . In these locations, we hypothesise that the grounding zone geometry is relatively immune to dynamic thinning, and that the GL subsequently advanced in response to the high rates of accumulation experienced by the BSS [Lenaerts et al., 2012].

Finally, we highlight the minor GL retreat experienced by the ice streams feeding Venable Ice Shelf, which appears at odds with recent observations that this ice shelf has experienced significant thinning since the 1990s [e.g. Pritchard et al., 2012; Paolo et al., 2015], likely forced by CDW accessing the ice-shelf cavity via Belgica Trough [see Figure 1; Graham et al., 2011]. Indeed, Paolo et al. [2015] report Venable Ice Shelf as having experienced the most dramatic thickness reduction of all Antarctic ice shelves over the period 1994-2012, thinning at a mean rate of  $36.1 \pm 4.4 \text{ m decade}^{-1}$  to 82% of its 1994 thickness. Despite this exceptional thinning, and known deep bathymetry to the ice shelf's northern margin that potentially connects to the CDW-flooded Belgica Trough, we have observed only limited GL retreat at this location. Here, the largest GL change occurred between 1985 and 1990 (0.22 km of retreat at  $45 \text{ m yr}^{-1}$ ; segments 30-32 in Data Set S1); and little change in GL position has been observed since. As noted previously, a small retreat is apparent in 2010-2015, but its magnitude (total 0.11 km) is insufficient to support a case that it represents a significant upward or persistent trend in retreat rate [cf. Wouters et al., 2015]. We propose that the discrepancy between oceanic forcing and suppressed GL response observed over the last two decades is a result of the specific bed geometry at/around the grounding zone, presently acting to pin the GL to its current location. Radar data acquired by NASA Operation

IceBridge suggest that the bed along the Venable Ice Shelf GL is relatively shallow, including where Wiesnet and Williams Ice Streams feed into the ice shelf (Figure 3). Significantly, however, where the same surveys profiled ice thickness inland, they partly captured a deep basin underlying Williams Ice Stream from ~40 km inland. A subsequent airborne gravity survey of this basin, reaching a further 50 km inland (Figure 3), showed free-air gravity anomalies 80-100 mGal lower than the surroundings, comparable to those observed over Ferrigno Ice Stream [Bingham et al., 2012], indicating the likely existence of a significant, deeply-bedded basin lying beneath Williams Ice Stream. This feature is not identified in Bedmap2 [Fretwell et al., 2013], which did not incorporate these gravity-anomaly data, and renders the setting analogous to both Ferrigno Ice Stream and Pine Island Glacier, which are already experiencing active dynamic thinning. Moreover, in the case of Pine Island Glacier, the current trends are a likely response to the floating section having become ungrounded from a previously longstanding pinning point [Jenkins et al., 2010]. We propose Williams Ice Stream, therefore, as an analogous setting with potential for significant future retreat once the coastal pinning point is breached. This hypothesis calls for much improved knowledge of the subglacial geometry of the GL at Williams Ice Stream/Venable Ice Shelf as an important scientific objective to facilitate numerical modelling of the region's future.

## 5. Conclusions

Our analysis of Landsat-derived grounding line change reveals that ~65% of the grounding line of the Bellingshausen Sea margin retreated between 1990 and 2015. The changes are pronounced, as expected, in locations where known bathymetric lows across the continental shelf facilitate ocean-driven dynamic thinning (e.g. Ferrigno Ice Stream), but have occurred

more pervasively along the entire coastline than has previously been reported, implicating the likely ingress of relatively warm circumpolar deep water to the majority of the Bellingshausen Sea margin. Nevertheless, despite extensive thinning over recent decades, we observe only minimal grounding line retreat at Venable Ice Shelf. Hypothesized to be currently pinned to a sub-ice topographic high, future sustained shelf thinning at or exceeding recently reported rates would breach this barrier and facilitate ice retreat into a significant inland basin, analogous to nearby Pine Island Glacier. Together, these findings warrant the requirement for continued observation of this important and dynamically evolving region of Antarctica.

### **Acknowledgements and Data**

FDWC was funded by a Carnegie Trust for the Universities of Scotland Carnegie-Caledonian Ph.D. Scholarship with RGB, hosted in the Edinburgh E3 U.K. Natural Environment Research Council Doctoral Training Partnership and the Scottish Alliance for Geoscience, Society and Environment Graduate School. NG was funded under the European Space Agency's Support to Science Elements CryoSat+ CryoTop study. Landsat data used in this study are available from the USGS/NASA at [earthexplorer.usgs.gov/](http://earthexplorer.usgs.gov/); SAR and Cryosat-2 data are available from the European Space Agency; IceBridge data were acquired as part of NASA's Operation IceBridge Project, and is available at: [nsidc.org/icebridge/portal/](http://nsidc.org/icebridge/portal/). FDWC also acknowledges Geosoft Inc. for their contribution of Oasis Montaj & Geophysics licenses used to process gravity data. The authors declare no real or perceived conflicts of interests as a result of this paper. Supplementary data supporting the results of this paper are available in the accompanying supporting information file.

## References

- Bindschadler, R., et al. (2011), Getting around Antarctica: New high- resolution mappings of the grounded and freely-floating boundaries of the Antarctic Ice Sheet created for the International Polar Year, *Cryosphere*, 5, 569-588, <http://dx.doi.org/10.5194/tcd-5-183-2011>.
- Bingham, R.G., F. Ferraccioli, E.C. King, R.D. Larter, H.D. Pritchard, A.M. Smith, and D.G., and Vaughan (2012), Inland thinning of West Antarctic Ice Sheet steered along subglacial rifts, *Nature*, 487, 468-471, doi:10.1038/nature11292.
- Brunt, K., H.A. Fricker, L. Padman, T. Scambos, and S. O'Neel (2010), Mapping the grounding zone of the Ross Ice Shelf, Antarctica, ICESat laser altimetry, *Ann. Glaciol.*, 51, 71–79, doi:10.3189/172756410791392790.
- Brunt, K.M., H.A. Fricker, and L. Padman (2011), Analysis of ice plains of the Filchner-Ronne Ice Shelf, Antarctica, using ICESat laser altimetry, *J. Glaciol*, 57(205), 965-975.
- Cochran, J. R. and R. E. Bell (2010, updated 2014), *IceBridge Sander AIRGrav L1B Geolocated Free Air Gravity Anomalies*, digital media [subset IGGRV1B\_20121025\_11594800\_V016], Boulder, Colorado USA: NASA National Snow and Ice Data Center Distributed Active Archive Center. <http://dx.doi.org/10.5067/R1RQ6NRIJV89>.
- Cochran, J.R., S.S. Jacobs, K.J. Tinto, and R.E. Bell (2014), Bathymetric and oceanic controls on Abbot Ice Shelf thickness and stability, *Cryosphere*, 8, 877-889, doi:10.5194/tc-8-877-2014.

Corr, H.F.J., C.S.M. Doake, A. Jenkins, and D.G. Vaughan (2001), Investigations of an "ice plain" in the mouth of Pine Island Glacier, Antarctica, *J. Glaciol.*, 47(156), 51-57, doi:10.3189/172756501781832395.

Favier, L., G. Durand, S.L. Cornford, G.H Gudmundsson, O. Gagliardini, F. Gillet-Chaulet, T. Zwinger, A.J. Payne, and A.M. Le Brocq (2014), Retreat of Pine Island Glacier controlled by marine ice-sheet instability, *Nat. Clim. Chang.*, 4, 117-121, doi:10.1038/nclimate2094.

Ferrigno, J.G., A.J. Cook, A.M. Mathie, R.S. Williams, Jr., C. Swithinbank, K.M. Foley, A.J. Fox, J.W. Thomson, and J. Sievers (2009), Coastal-Change and Glaciological Map of the Palmer Land Area, Antarctica: 1947–2009 and accompanying explanatory pamphlet, US Geological Survey, USA, *Geologic Investigations Series Map I-2600-C*.

Fretwell, P., et al. (2013), Bedmap2: Improved ice bed, surface and thickness datasets for Antarctica, *Cryosphere*, 7, 375–393, doi:10.5194/tc-7-375-2013.

Fricker, H.A., Coleman, R., Padman, L., Scambos, T.A., Bohlander, J. and Brunt, K.M (2009), Mapping the grounding zone of the Amery Ice 422 Shelf, East Antarctica using DInSAR, MODIS and ICESat, *Antarct. Sci.*, 21(5), 515–532, doi:10.1017/S095410200999023X.

Fricker, H.A. and L. Padman (2006), Ice shelf grounding zone structure from ICESat laser altimetry, *Geophys. Res. Lett.*, 33(15), L15502, doi:10.1029/2006GL026907.

Goldberg, D.N., P. Heimbach, I. Joughin, and B. Smith (2015), Committed retreat of Smith, Pope, and Kohler Glaciers over the next 30 years inferred by transient model calibration, *Cryosphere*, 9, 2429-2446, doi:10.5194/tc-9-2429-2015.

Graham, A.G.C., R.D. Larter, and F.O. Nitsche (2011), An improved bathymetry compilation for the Bellingshausen Sea, Antarctica, to inform ice sheet and ocean models, *Cryosphere*, 5, 95-106, doi:10.5194/tc-5-95-2011.

Gray, L., D. Burgess, L. Copland, R. Cullen, N. Galin, R. Hawley, and V. Helm (2013), Interferometric swath processing of CryoSat-2 data for glacial ice topography, *Cryosphere*, 7, 1857-1867.

Haran, T., J. Bohlander, T. Scambos, T. Painter, and M. Fahnestock (2005, updated 2013), *MODIS Mosaic of Antarctica 2003-2004 (MOA2004) Image Map, digital media*, Boulder, Colorado, USA: National Snow and Ice Data Center. <http://dx.doi.org/10.7265/N5ZK5DM5>.

Haran, T., J. Bohlander, T. Scambos, T. Painter, and M. Fahnestock (2014), *MODIS Mosaic of Antarctica 2008-2009 (MOA2009) Image Map*, digital media, Boulder, Colorado, USA: National Snow and Ice Data Center. <http://dx.doi.org/10.7265/N5KP8037>.

Hawley, R. L., A. Shepherd, R. Cullen, V. Helm, and D. J. Wingham (2009), Ice-sheet elevations from across-track processing of airborne interferometric radar altimetry, *Geophys. Res. Lett.*, 36, L22501.

Holt, T.O., H.A. Fricker, N.F. Glasser, O. King, A. Luckman, L. Padman, D.J Quincey, and M.R. Siegfried (2014), The structural and dynamic responses of Stange Ice Shelf to recent environmental change, *Antarct. Sci.*, 26(6), 646-660, doi:10.1017/S095410201400039X.

Jenkins, A., et al. (2010), Observations beneath Pine Island Glacier in West Antarctica and implications for its retreat, *Nat. Geosci.*, 3(7), 468-472, doi:10.1038/ngeo890.

Jacobs, S.S., A. Jenkins, C.F. Giulivi and P. Dutrieux (2011), Stronger ocean circulation and increased melting under Pine Island Glacier ice shelf, *Nat. Geosci.*, 4, 519-523, doi:10.1038/ngeo1188.

Joughin, I., R.B. Alley, and D.M. Holland (2012), Ice-Sheet Response to Oceanic Forcing, *Science*, 38, 1172-1176, doi:10.1126/science.1226481.

Joughin, I., B.E. Smith, and B. Medley (2014) Marine ice sheet collapse potentially under way for the Thwaites Glacier basin, West Antarctica, *Science*, 344(6185), 735-738, doi: 10.1126/science.1249055.

Lee, D.S., J.C. Storey, M.J. Choate, and R.W. Hayes (2004), Four Years of Landsat-7 On-Orbit Geometric Calibration and Performance, *IEEE Trans. Geosci. Remote Sens.*, 42(12), 2786-2795, doi:10.1109/TGRS.2004.836769.

Lenaerts, J.T.M., M.R. van den Broeke, W.J. van de Berg, E. van Meijgaard, and P. Kuipers Menneke (2012) A new, high-resolution surface mass balance map of Antarctica (1979-2010) based on regional atmospheric climate modelling, *Geophys. Res. Lett.*, 39(4), GL050713, doi: 10.1029/2011GL050713.

Leuschen, C., P. Gogineni, F. Rodriguez-Morales, J. Paden, and C. Allen (2010a, updated 2015a), *IceBridge MCoRDS L2 Ice Thickness, Version 1, digital media* [subset IRMCR\_20091103\_02], Boulder, Colorado, USA. NASA National Snow and Ice Data Center Distributed Active Archive Center. <http://dx.doi.org/10.5067/GDQ0CUCVTE2Q>.

Leuschen, C., P. Gogineni, F. Rodriguez-Morales, J. Paden, and C. Allen (2010b, updated 2015b), *IceBridge MCoRDS L2 Ice Thickness, Version 1, digital media* [subset IRMCR2\_20111116\_02], Boulder, Colorado, USA. NASA National Snow and Ice

<http://dx.doi.org/10.5067/GDQ0CUCVTE2Q>.

MacGregor, J.A., G.A. Catania, M.S. Markowski and A.G. Andrews (2012), Widespread rifting and retreat of ice-shelf margins in the eastern Amundsen Sea Embayment between 1972 and 2011, *J. Glaciol*, 58(209), 458-466, doi: 10.3189/2012JoG11J262.

McMillan, M., A. Shepherd, A. Sundal, K. Briggs, A. Muir, A. Ridout, A. Hogg, and D. Wingham (2014), Increased ice losses from Antarctica detected by CryoSat-2, *Geophys. Res. Lett.*, 41(11), 3988-3905, doi:10.1002/2014GL060111.

Ó Cofaigh, C.O., J.A. Dowdeswell, J. Evans, C-D. Hillenbrand, R.D. Larter, P. Morris, and C.J. Pudsey (2005), Flow of the West Antarctic Ice Sheet on the continental margin of the Bellingshausen Sea at the Last Glacial Maximum, *J. Geophys. Res.*, 110, b11103, doi:10.1029/2005jb003619.

Paolo, F.S., H.A. Fricker, and L. Padman (2015), Volume loss from Antarctic ice shelves is accelerating, *Science*, 348, 327-331, doi:10.1126/science.aaa0940.

Park, J. W., N. Gourmelen, A. Shepherd, S. W. Kim, A. Vaughan, and D. G. Wingham (2013), Sustained retreat of the Pine Island Glacier, *Geophys. Res. Lett.*, 40, 2137–2142, doi:10.1002/grl.50379.

Pritchard, H. D., R. J. Arthern, D. G. Vaughan, and L. A. Edwards (2009), Extensive dynamic thinning on the margins of the Greenland and Antarctic ice sheets, *Nature*, 461, 971–975, doi:10.1038/nature08471.

Pritchard, H.D., S.R.M. Ligtenberg, H.A. Fricker, D.G. Vaughan, M.R. van den Broeke, and L. Padman (2012), Antarctic ice sheet loss driven by basal melting of ice sheets, *Nature*, 484, 502-505, doi:10.1038/nature10968.

- Rignot, E., J. L. Bamber, M. R. van den Broeke, C. Davis, Y. Li, W. J. van de Berg, and E. van Meijgaard (2008), Recent Antarctic ice mass loss from radar interferometry and regional climate modelling, *Nat. Geosci.*, *1*, 106–110, doi:10.1038/ngeo102.
- Rignot, E., J. Mouginot, and B. Scheuchl (2011), Antarctic grounding line mapping from differential satellite radar interferometry, *Geophys. Res. Lett.*, *38*, L10504, doi:10.1029/2011GL047109.
- Rignot, E., J. Mouginot, M. Morlighem, H. Seroussi, and B. Scheuchl (2014), Widespread, rapid grounding line retreat of Pine Island, Thwaites, Smith, and Kohler glaciers, West Antarctica, from 1992 to 2011, *Geophys. Res. Lett.*, *41*(10), 3502-3509, doi:10.1002/2014GL060140.
- Scambos, T.A., T.M. Haran, M.A. Fahnestock, T.H. Painter, and J. Bohlander (2007), MODIS-based Mosaic of Antarctica (MOA) data sets: Continent-wide surface morphology and snow grain size, *Remote Sens. Environ.*, *111*, 242–257, doi:10.1016/j.rse.2006.12.020.
- Scott, J.B.T., G.H. Gudmundsson, A.M. Smith, R.G. Bingham, H.D. Pritchard, and D.G. Vaughan (2009), Increased rate of acceleration on Pine Island Glacier strongly coupled to changes in gravitational driving stress, *Cryosphere*, *3*, 125-131, doi:10.5194/tc-3-125-2009.
- Seroussi, H., M. Morlighem, E. Rignot, J. Mouginot, E. Larour, M. Schodlok, and A. Khazendar (2014), Sensitivity of the dynamics of Pine Island Glacier, West Antarctica, to climate forcing for the next 50 years, *Cryosphere*, *8*, 1699-1710, doi:10.5194/tc-8-1699-2014.
- Shepherd, A., D. Wingham, and E. Rignot (2004), Warm ocean is eroding West Antarctic Ice Sheet, *Geophys. Res. Lett.*, *31*(23), L23402, doi:10.1029/2004GL021106.

Shepherd, A., D. Wingham, D. Wallis, K. Giles, S. Laxon, and A.V. Sundal (2010), Recent loss of floating ice and the consequent sea level contribution, *Geophys. Res. Lett.*, *37*(13), L13503, doi:10.1029/2010GL042496.

Shepherd, A. et al. (2012), A Reconciled Estimate of Ice-Sheet Mass Balance, *Science*, *338*(6111), 1183-1189, doi:10.1126/science.1228102.

Storey, J., M. Choate, and K. Lee (2014), Landsat 8 Operational Land Imager On-Orbit Geometric Calibration and Performance, *Remote Sens.*, *6*(11), 11127-11152, doi:10.3390/rs6111127.

Swithinbank, C., R.S. Williams, Jr., J.G. Ferrigno, K.M. Foley, C.E. Rosanova, and L.M. Dailide (2004), Coastal-change and glaciological map of the Eights coast area, Antarctica: 1972–2001 and accompanying explanatory pamphlet, US Geological Survey, USA, *Geologic Investigations Series Map I-2600-E*.

Tucker, C.J., D.M. Grant, and J.D. Dykstra, (2004), NASA's Global Orthorectified Landsat Data Set Compton, *Photogramm. Eng. Remote Sens.*, *70*(3), 313-322, doi:10.14358/PERS.70.3.313.

Vaughan, D.G., J.C. Comiso, I. Allison, J. Carrasco, G. Kaser, R. Kwok, P. Mote, T. Murray, F. Paul, J. Ren, E. Rignot, O. Solomina, K. Steffen, and T. Zhang (2013), Observations: Cryosphere, In: *Climate Change 2013: The Physical Science Basis. Contribution of Working Group I to the Fifth Assessment Report of the Intergovernmental Panel on Climate Change*, 317-382, Cambridge University Press, Cambridge, United Kingdom and New York, NY, USA.

Walker, D.P., M.A., Brandon, A. Jenkins, J.T., Allen, J.A. Dowdeswell, and J. Evans (2007),

Oceanic heat transport onto the Amundsen Sea shelf through a submarine glacial trough, *Geophys. Res. Lett.*, *34*, L02602, 1-4, doi:10.1029/2006GL028154.

Williams, C.R., R.C.A. Hindmarsh, and R.J. Arthern (2014), Calculating balance velocities

with a membrane stress correction, *J. Glaciol.*, *60*(220), 294-304, doi:10.3189/2014JoG13J092.

Wouters, B., A. Martin-Español, V. Helm, T. Flament, J. M. van Wessem, S. R. M.

Ligtenberg, M. R. van den Broeke, and J. L. Bamber (2015), Dynamic thinning of glaciers on the Southern Antarctic Peninsula, *Science*, *348*, 899-903, doi:10.1126/science.aaa5727.

Accepted Article



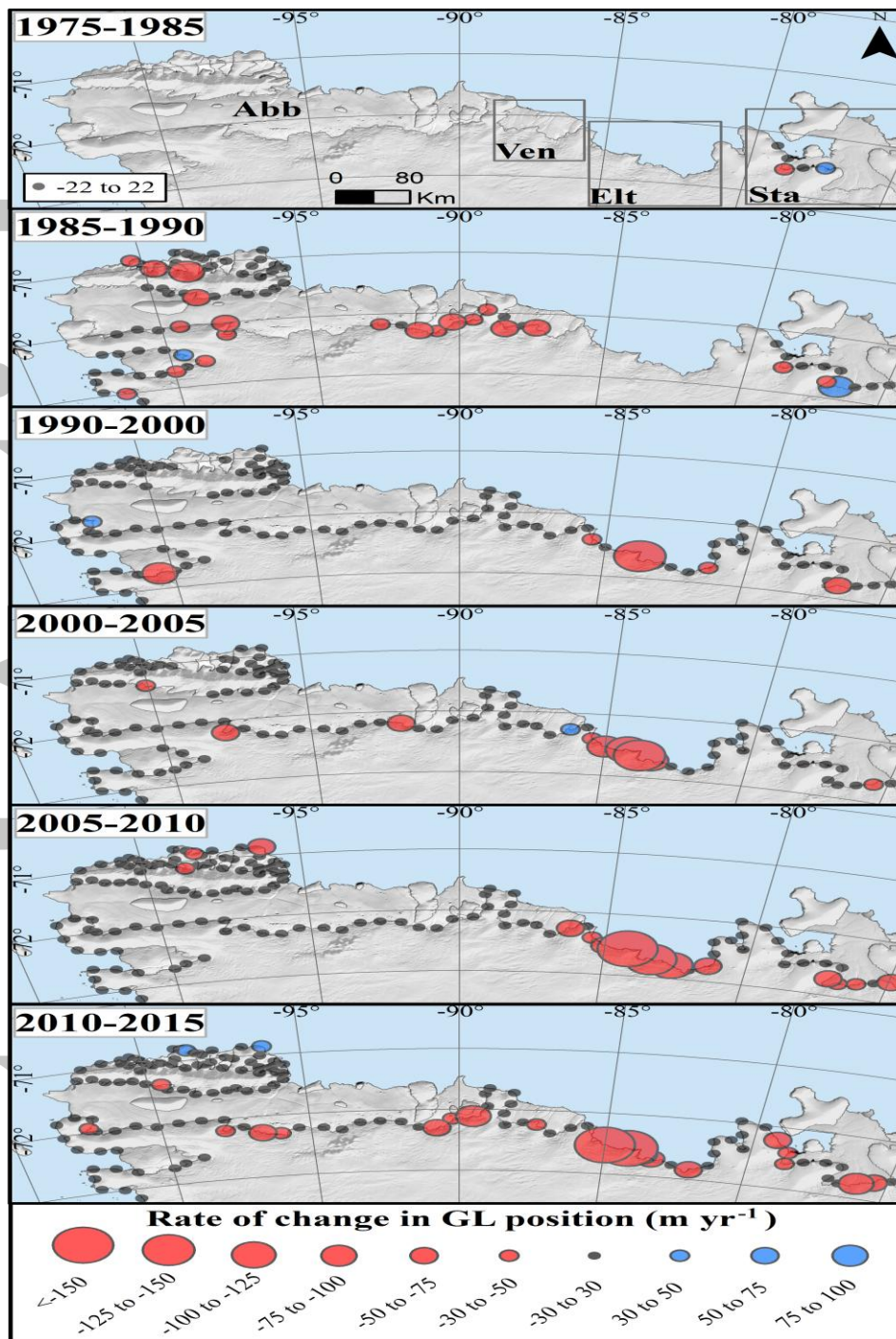


**Figure 2.** Rate of change in GL position over 5-10 year epochs between 1975 and 2015. Circle radii denote the magnitude and direction of change (red: *retreat*, blue: *advance*) for every 30 km segment; black circles indicate changes within Landsat error bounds. Note the non-linear scaling of change, and different scale for 1975-1985 error bounds. Site labels as per Figure 1. Data overlaid upon MOA2004 [Haran et al., 2013].

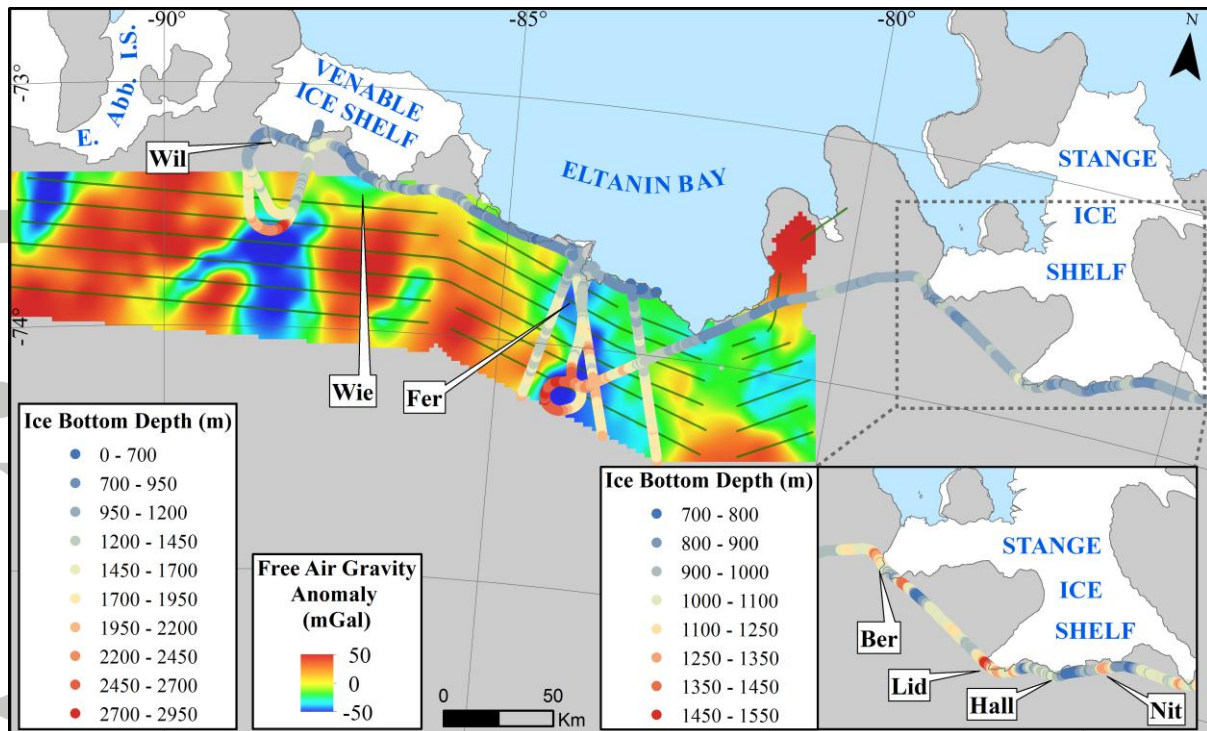


**Figure 3.** IceBridge radar and gridded free-air gravity anomaly data over the eastern BSS.

Radar profiles were acquired on 3 November 2009 and 16 November 2011 [Leuschen et al., 2015a, 2015b]; gravity data were acquired on 25 October 2012 (flight-lines in green) [Cochran & Bell, 2014]. *E. Abb. I.S.* denotes eastern Abbot Ice Shelf. Inset shows enlarged radar-derived ice bottom depths at Stange Ice Shelf. All other site labels as per Figure 1. Black lines delineate the 2008/2009 MOA GL [Haran et al., 2014].

Accepted